Pseudomorphic Synthesis of Large-Particle Co−MCM-41

Sangyun Lim, Alpana Ranade, Guoan Du, Lisa D. Pfefferle, and Gary L. Haller*

Department of Chemical Engineering, Yale University, P.O. Box 208286, New Haven, Connecticut 06520-8286

Received June 8, 2006. Revised Manuscript Received September 4, 2006

Large-particle (15 and 40 μm) Co−MCM-41 was synthesized using a pseudomorphic transformation. To maintain the spherical shape of the parent silica particles, overcondensation of silanol groups has to be avoided under a moderately basic synthesis condition. After 4 days of autoclaving at 100 °C with the Co−MCM-41 synthesis solution of which the initial pH was adjusted to 12.0, nonruptured spherical Co−MCM-41 particles, having one-dimensional pores in which Co ions are highly dispersed, were successfully synthesized. The reduction stability of this catalyst was affected by Co ion location controlled by pH adjustment and hydrogen spillover from residual cobalt oxide on the surface, which had not been incorporated into the silica matrix.

Introduction

Metal ion incorporated MCM-41 is a useful and effective catalyst for various catalytic reactions. The flexible framework (noncrystalline) structure of MCM-41 enables relatively facile introduction of a broad range of metal ions without structural collapse. Isomorphous substitution of Si by various metal ions of substantially improved physicochemical stability of active components has resulted in improved catalysts for several reactions.[1−6]However, small particle size with extremely high porosity, which results from the initial silica sources, may present unexpected challenges. For example, the low bulk density of Co−MCM-41 is a major barrier for use in a fluidized-bed reactor. A fluidized-bed reactor is considered as a promising approach for the catalytic growth of carbon nanotubes on a large scale with a uniform bed temperature distribution. For templated growth of a nanostructure, i.e., BMg and GaN, fewer defects and longer length are required to obtain the expected electrochemical properties. To satisfy these requirements, metal ion incorporated MCM-41 with large spherical particles consisting of pores all the way through the particle with uniform distribution of metal ions is required.

The concept of pseudomorphism may be a synthesis approach for large-particle MCM-41 catalyst applications. A pseudomorph, in mineralogy, is a crystal or other body consisting of one mineral but having the form or shape of another, a consequence of having been formed by substitution, or by chemical or physical alteration. In this study, MCM-41 particles can be considered as pseudomorphs of the silica gel grains used in the synthesis. Each silica grain can behave like a microreactor in which silica may be dissolved by the alkaline solution, and silica species interact with surfactant to form the MCM-41 pore structure, as in the usual synthesis procedure. Pseudomorphic synthesis of pure siliceous MCM-41 using large silica particles, 5−15 μm in diameter, was first introduced by Martin et al. in 2002,[7] applied to a separation medium,[8] and expanded to MCM-48.[9] These processes are for pure siliceous mesoporous materials and utilize NaOH. However, for the application to MCM-41 as a catalytic material, metal ion incorporated MCM-41, sodium has a negative effect in the substitution of metal ions and catalytic reaction, as well as stability. Uniform distribution of metal ions through the pore surface is a key property in the metal ion incorporated MCM-41 compared to pure siliceous MCM-41.

In this study, therefore, a non-sodium process is introduced for the pseudomorphic synthesis of Co−MCM-41, which may be applied to a wide range of metal ions. The physical and chemical properties were investigated by temperature programmed reduction (TPR), nitrogen physisorption, and scanning electron micrograph (SEM) to suggest a set of preferred synthesis conditions for obtaining a successful Co−MCM-41 pseudomorph.

Experimental Section

A non-sodium process was used to synthesize Co−MCM-41 following the detailed synthesis procedure described elsewhere.[10,11]

* To whom correspondence should be addressed. E-mail: gary.haller@yale.edu.

(1) Du, G. A.; Lim, S. Y.; Yang, Y. H.; Wang, C.; Pfefferle, L.; Haller, G. L. *Appl. Catal., A* **2006**, *302*, 48.
(2) Yang, Y.; Du, G.; Lim, S.; Haller, G. L. *J. Catal.* **2005**, *234*, 318.
(3) Chen, Y.; Ciuparu, D.; Yang, Y.; Lim, S.; Wang, C.; Haller, G. L.; Pfefferle, L. *Nanotechnology* **2005**, *16*, S476.
(4) Chen, Y.; Ciuparu, D.; Lim, S. Y.; Yang, Y. H.; Haller, G. L.; Pfefferle, L. *J. Catal.* **2004**, *225*, 453.
(5) Chen, Y.; Ciuparu, D.; Lim, S.; Yang, Y. H.; Haller, G. L.; Pfefferle, L. *J. Catal.* **2004**, *226*, 351.
(6) Lim, S.; Ciuparu, D.; Pak, C.; Dobek, F.; Chen, Y.; Harding, D.; Pfefferle, L.; Haller, G. *J. Catal. B* **2003**, *107*, 11048.
(7) Martin, T.; Galarneau, A.; Di Renzo, F.; Fajula, F.; Plee, D. *Angew. Chem., Int. Ed.* **2002**, *41*, 2590.
(8) Martin, T.; Galarneau, A.; Di Renzo, F.; Brunel, D.; Fajula, F.; Heinisch, S.; Cretier, G.; Rocca, J. L. *Chem. Mater.* **2004**, *16*, 1725.
(9) Petitto, C.; Galarneau, A.; Driole, M. F.; Chiche, B.; Alonso, B.; Di Renzo, F.; Fajula, F. *Chem. Mater.* **2005**, *17*, 2120.
(10) Lim, S.; Yang, Y. H.; Ciuparu, D.; Wang, C.; Chen, Y.; Pfefferle, L.; Haller, G. L. *Top. Catal.* **2005**, *34*, 31.
(11) Lim, S.; Ciuparu, D.; Chen, Y.; Yang, Y. H.; Pfefferle, L.; Haller, G. L. *J. Phys. Chem. B* **2005**, *109*, 2285.

10.1021/cm061342s CCC: $33.50
Published on Web 10/24/2006

Table 1. Sample List Investigated in This Study

samples[a]	size (μm)	cobalt source	sodium yes/no	autoclaving time (days)	initial pH	silica source
SI-1	15					
SI-2	40					
CM-1	15	sodium hexanitro cobaltate	Y	1		SI-1
CM-2	15	cobalt sulfate	Y (NaOH)	1		SI-1
CM-3	15	cobalt sulfate	N	6	11.5	SI-1 and TMASi[b]
CM-4	40	cobalt sulfate	N	6	11.5	SI-2 and TMASi[b]
CM-5	15	cobalt sulfate	N	4	12.0	SI-1 and TMASi[b]
CM-6	15	cobalt sulfate	N	4	11.5	SI-1 and TMASi[b]
CM-7	15	cobalt sulfate	N	4	11.0	SI-1 and TMASi[b]
CM-8	15	cobalt sulfate	N	4	10.5	SI-1 and TMASi[b]
CM-9	0.2−0.3	cobalt sulfate	N	6	11.5	Cab-O-Sil

[a] SI-1: 15 μm parental silica; SI-2: 40 μm parental silica; CM-1: Co−MCM-41 synthesized using sodium hexanitro cobaltate as cobalt source, autoclaved for 1 day at 100 °C; CM-2: Co−MCM-41 synthesized using sodium hydroxide, autoclaved for 1 day at 100 °C; CM-3: Co−MCM-41 synthesized using SI-1 as a silica source, non-sodium process, initial pH = 11.5, autoclaved for 6 days at 100 °C; CM-4: Co−MCM-41 synthesized using SI-2 as a silica source, non-sodium process, initial pH = 11.5, autoclaved for 6 days at 100 °C; CM-5: Co−MCM-41 synthesized using SI-1 as a silica source, non-sodium process, initial pH = 12.0, autoclaved for 4 days at 100 °C; CM-6: Co−MCM-41 synthesized using SI-1 as a silica source, non-sodium process, initial pH = 11.5, autoclaved for 4 days at 100 °C; CM-7: Co−MCM-41 synthesized using SI-1 as a silica source, non-sodium process, initial pH = 11.0, autoclaved for 4 days at 100 °C; CM-8: Co−MCM-41 synthesized using SI-1 as a silica source, non-sodium process, initial pH = 10.5, autoclaved for 4 days at 100 °C; CM-9: Co−MCM-41 synthesized using Cab-O-Sil as a silica source, non-sodium process, initial pH = 11.5, autoclaved for 6 days at 100 °C. [b] TMASi is tetramethylammonium silicate, $(CH_3)_4NOH{\cdot}2SiO_2$

Two different sizes of spherical silica, 15 μm (99.99% SiO_2, Kromasil, Eka Chem.) and 40 μm (99.9% SiO_2, Fluka), were used as parent silica, and the resulting samples were compared to the sample synthesized using fumed silica, Cab-O-Sil (Sigma-Aldrich, 0.2−0.3 μm). All the Co−MCM-41 catalysts have the same chemical composition ratio, which is Si:Co:surfactant:H_2O = 1:0.01:0.27:86. Two sodium-containing samples were also prepared as reference samples using NaOH and sodium hexanitro cobaltate ($Na_3Co(NO_2)_6$, Sigma-Aldrich), following the recipe reported by Martin et al.[7] Table 1 shows a list of the synthesized samples in this study, and each sample's name was symbolized for convenience. Effects of particle size and initial pH of the synthesis solution were investigated by assessing the reduction properties and stability, physical structure, and morphology using TPR, N_2 physisorption, and SEM, respectively.

The reduction stability and properties of the Co−MCM-41 samples were investigated by a hydrogen TPR technique using a thermal conductivity detector (TCD) of a gas chromatograph (6890 plus, Agilent). Approximately 200 mg of each sample was loaded into a quartz cell. Prior to each TPR run, the sample cell was purged by ultra zero grade air at room temperature, and then the temperature was increased to 500 °C at 5 °C/min, soaked for 1 h at the same temperature, and cooled to room temperature. This procedure produces a clean surface with a uniform degree of dehydration before running the TPR. The gas flow was switched to 5% hydrogen in argon balance, and the baseline was monitored until stable. After baseline stabilization, the sample cell was heated at 5 °C /min up to 850 °C and held for 1 h at the same temperature to ensure complete cobalt reduction. An acetone-dry ice trap was installed between the sample cell and the TCD to condense water, produced by sample reduction.

Nitrogen physisorption was carried out at −196 °C with a static volumetric instrument Autosorb-3B (Quantachrome) to obtain physical information on the Co−MCM-41 samples synthesized under different conditions. Prior to measurement, the samples were outgassed at 200 °C to a residual pressure below 1×10^{-4} Torr. A Baratron pressure transducer (0.001−10 Torr) was used for low-pressure measurements. The pore volume and porosity were calculated from the desorption isotherms using the BJH method. Although the BJH method underestimates the mesopore size, the pore size distribution determined in our study provides reliable results that can be used for the relative comparison of the synthesized samples.[6]

The morphology of Co−MCM-41 pseudomorphs and parent silica was observed by SEM (XL-30 ESEM-FEG, FEI Company) analysis. All samples were coated with gold for 10 min (about 10 nm of gold film thickness) before analysis. The acceleration voltage was 10 kV, and the spot size was 3 with 10 ± 0.3 mm of working distance.

Results and Discussion

As mentioned above, the presence of Na cations has a negative effect on the incorporation of some heteroatoms in the silica framework.[12] For the synthesis of single-wall carbon nanotubes (SWNT), the uniform distribution of a single species of Co ion (Co^{2+}) in the silica framework is critical because the quality of carbon nanotubes is directly related to the reducibility of Co ions. The existence of Na ions in the synthesis solution may cause inhomogeneous incorporation of Co ions in the framework, resulting in different species of Co having different reduction stability. This heterogeneity in the reduction properties produces different sizes of carbon nanotubes and shows low selectivity to SWNT. The importance of the chemical purity was discussed in detail elsewhere.[10]

To investigate the effect of sodium ions on the reduction behavior of Co−MCM-41, two sodium-containing Co−MCM-41 samples were synthesized following Martin et al.[7] The chemical properties and reduction behavior were the priorities of this study. Figure 1 shows the hydrogen TPR results of the sodium-containing Co−MCM-41 samples, CM-1 and CM-2, and non-sodium-containing Co−MCM-41 samples, CM-3, CM-4, and CM-9. (For a detailed description of the sample symbols, see Table 1.) When the samples contain sodium, CM-1 and CM-2, there are two different distinct reduction peaks in the reduction range of non-sodium samples, indicating nonhomogeneous distribution of cobalt ions in the sample. This may be attributed to the competition in the isomorphous substitution of silica between Co and sodium ions during the synthesis procedure. Nonhomogeneity in reduction of Co−MCM-41 produces multiple sizes of cobalt metal clusters on the surface under the reaction conditions of SWNT, resulting in a broad range

(12) Pena, M. L.; Kan, Q.; Corma, A.; Rey, F. *Microporous Mesoporous Mater.* **2001**, *44*, 9.

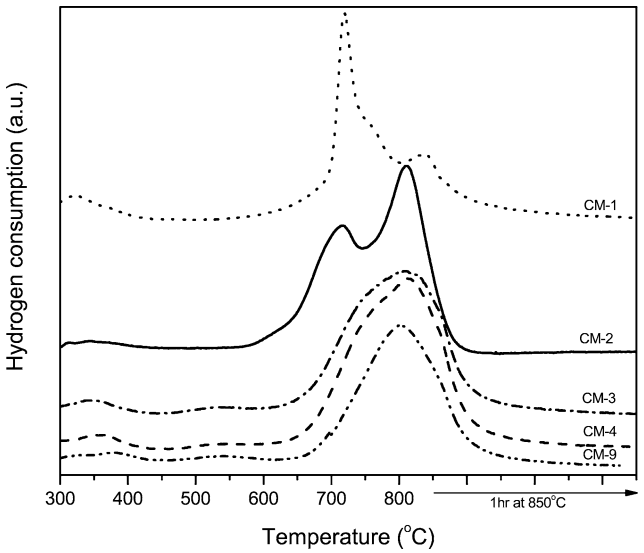

Figure 1. Hydrogen temperature-programmed reduction (TPR) profiles of Co−MCM-41 samples synthesized pseudomorphically. (For sample identification, see Table 1.)

of tube sizes and/or showing low selectivity for SWNT. Therefore, the sodium-containing samples are excluded from further consideration here. On the other hand, Co−MCM-41 pseudomorphs synthesized by a non-sodium-containing method, CM-3 and CM-4, show the same homogeneous reduction patterns of Co^{2+} ions as the sample used for the synthesis of high-quality SWNT earlier, CM-9.[4−6,13] This suggests that Co−MCM-41 pseudomorphs may be directly applied to the synthesis of SWNT.

Nitrogen physisorption was performed with CM-3 and CM-4, and the results were compared to those of the parent silicas, SI-1 and SI-2, as shown in Figure 2. Spherical parent silica having diameters of 15 and 40 μm show a broad pore size distribution because there is no regular structure developed inside the particles. However, after autoclaving for 6 days with a templating material and pH adjustment, a distinct capillary condensation appears in the isotherms and a narrow pore size distribution developed, which averaged around 30 Å regardless of the particle size. This indicates, at least from the physical point of view, that a successful synthesis of Co−MCM-41 has been achieved, and pseudomorphs are confirmed by the SEM morphology. There is no visual difference in the nitrogen physisorption results of CM-3 and CM-4, although the parent silica of two samples has different particle sizes and physical structure inside the silica spheres, as shown in Figure 2. The nitrogen adsorption volume of CM-3 and CM-4 near $p/p_o = 1$ increases as compared to that of the parent silica, which may be due to newly created interparticle space caused by rupture of some spherical particles after 6 days of autoclaving. Each particle behaves like a microreactor in which silica is dissolved by the basic solution and silicate species interact with the surfactant to form the MCM-41 structure.[7] If the autoclaving time is too long, the spherical structure may be destroyed by overcondensation of the silanol groups, and this also can happen at high pH of the initial solution. Therefore, simultaneous control of condensation time and the initial pH of the synthesis solution is critical. For a parent silica with a low initial pore volume, the particles cannot accommodate the formation of MCM-41 and burst during the synthesis.[7] The pore volumes of parent silica used in this study were 1.29 cm^3/g for SI-1 and 0.87 cm^3/g for SI-2, which are greater than those reported elsewhere.[7] Thus, only autoclaving time and pH effects are considered in this study. Figure 3, SEM pictures of the parent silica and the Co−MCM-41 pseudomorphs, confirm particle rupture as a result of overcondensation of silanol groups. The sodium-containing samples, CM-1 and CM-2, show a significant amount of amorphous silica resulting from particle rupture under a highly basic synthesis condition, although these samples were autoclaved for only 1 day. This amorphous silica contributes to the increase of nitrogen adsorption volume at a high relative pressure. By a simple nitrogen physisorption, therefore, the degree of rupture of spherical silica can be estimated.

To avoid particle rupture by overcondensation and highly basic conditions, 4 days of autoclaving was utilized instead of 6 days, and the initial pH of the Co−MCM-41 synthesis solution was adjusted from 10.5 to 12.0 in steps of 0.5. Figure 4 shows SEM images of these samples (CM-5, CM-6, CM-7, and CM-8) compared to the parent silica (SI-1) and CM-3 (initial pH = 11.5 and autoclaved for 6 days). All four Co−MCM-41 samples (CM-5, CM-6, CM-7, and CM-8) maintain the morphology of the parent silica without significant rupture, which can be clearly distinguished from CM-3 (Figure 4b). Less deformation of particles can be noted as the initial pH decreases, which was as predicted. However, less dissolution of silica inside the particle might happen under lower pH, resulting in incomplete formation of Co−MCM-41 physically and chemically. Therefore, further characterizations of these samples were performed using nitrogen physisorption for physical properties and hydrogen TPR for chemical properties.

Nitrogen physisorption, as shown in Figure 5, was performed for Co−MCM-41 pseudomorphs synthesized under the different initial pH for 4 days and compared with parent silica (SI-1). Parent silica shows a hysteresis loop around a relative pressure equal to 0.7, which represents typical ink-bottle-shaped pores. There is no further physisorption at high relative pressure, caused by interparticle space, because of the clean spherical shape, as seen in SEM images. If, therefore, there were particle rupture, random shapes of amorphous silica would create space between particles, resulting in adsorption volume increase at high relative pressure. Parent silica also shows a broad pore size distribution, showing the highest fraction around 80 Å. However, after a successful pseudomorphic synthesis of Co−MCM-41, the maximum volume fraction of the pore size shifted to 30 Å, showing a narrow distribution. Figure 5a does not show a sudden increase in adsorption volume, regardless of the initial pH, in the high relative pressure range unlike the samples autoclaved for 6 days (Figure 2), suggesting no significant particle rupture. Another parameter measurable from the isotherm shape is the degree of mesopore formation inside the spherical particles. If mesopores are not formed completely through the inside particles,

(13) Ciuparu, D.; Chen, Y.; Lim, S.; Yang, Y. H.; Haller, G. L.; Pfefferle, L. *J. Phys. Chem. B* **2004**, *108*, 15565.

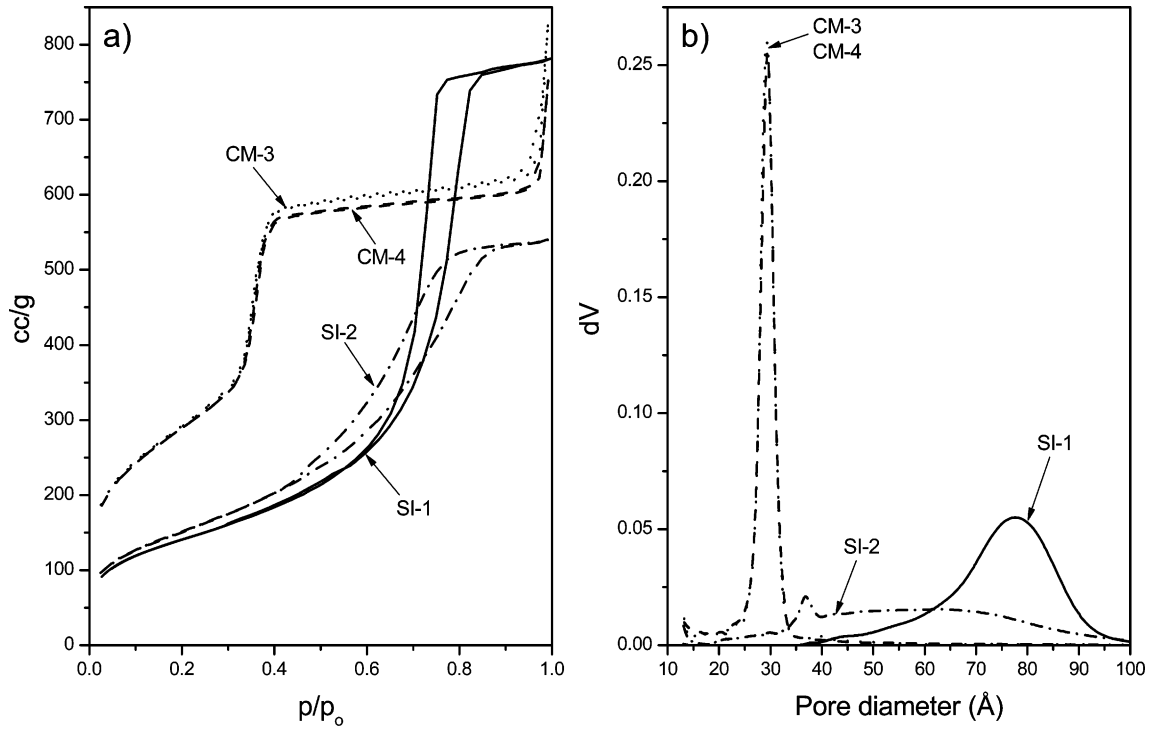

Figure 2. Nitrogen physisorption results of parent silica and Co−MCM-41 pseudomorphs. (For sample identification, see Table 1.)

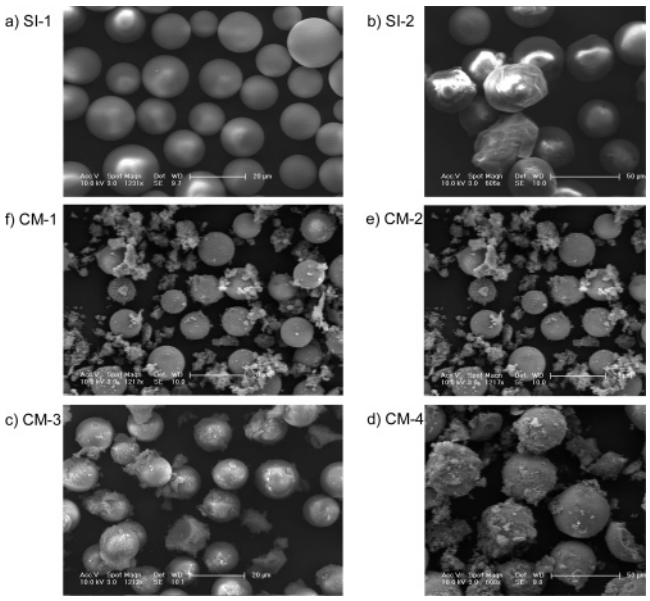

Figure 3. Scanning electron micrograph (SEM) images of Co−MCM-41 pseudomorphs and parent silica. (For sample identification, see Table 1.)

a mixture of ink-bottle-shaped pores of parent silica and one-dimensional mesopores of MCM-41, the isotherm would show both short capillary condensation and a hysteresis loop from MCM-41 and parent silica, respectively. The samples synthesized under the initial pH from 10.5 to 11.5 (CM-8, CM-7, and CM-6) show both capillary condensations and hystereses, indicating incomplete MCM-41 pore structure formed inside the particle. However, CM-5, synthesized at the initial pH = 12, shows no hysteresis and a large, steep capillary condensation step without the sudden increase of adsorption volume at high relative pressure, suggesting most of the amorphous silica inside the particle was transformed to a one-dimensional MCM-41 pore structure after 4 days' autoclaving. This sample also shows the narrowest (full-width at half-maximum, fwhm = 2 Å) and the highest volume fraction of pore size around 30 Å with unimodal pore size distribution; CM-6, CM-7, and CM-8 exhibit a bimodal pore size distribution attributed to the effect of unreacted parent silica. Of course, the pseudocrystalline pore structure can also be confirmed by XRD, which is illustrated for CM-5, see Figure 6. These results demonstrate that the optimum pseudomorphic synthesis conditions of Co−MCM-41 without particle rupture is 4 days of autoclaving under an initial pH of 12.

Table 2 shows the physical properties of Co−MCM-41 pseudomorphs and parent silica, which gives an idea of the completeness of pseudomorphic transformation of the parent silica. The surface area of parent silicas, SI-1 and SI-2, was just above 500 m^2/g, and it increases after pseudomorphic transformation under different synthesis conditions. The samples synthesized under the initial pH of 10.5 and 11.0 for 4 days show the lowest surface areas with the smallest mesoporosities. Mesoporosity was calculated from the ratio between mesopore volume (pore volume of pores under 10 nm of pore diameter) and total pore volume. As predicted in the nitrogen physisorption, mesoporosity of CM-5 shows the highest value (94%) and is almost the same value as the parent silica (96%), which suggests a complete transformation from parent silica to the MCM-41 structure, and results in the highest surface area (1159 m^2/g). When the particles are ruptured (CM-3 and CM-4) or incompletely transformed (CM-6, CM-7, and CM-8), the mesoporosity cannot reach the value of the parent silica. This suggests that each spherical silica particle was transformed into a MCM-41 structure, and the pores of MCM-41 are all the way through the particle. Because high dispersion of Co ions through the pores of MCM-41 has been proved,[6,11] homogeneous dispersion of Co ions within the spherical particle along the pore walls may be possible. This may make it possible to use pseudo-

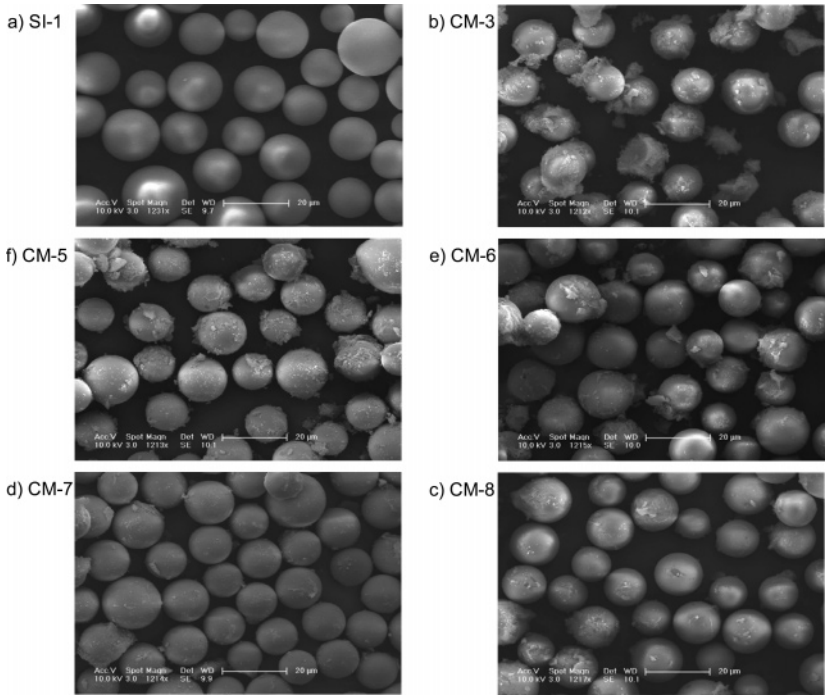

Figure 4. Scanning electron micrograph (SEM) images of Co−MCM-41 pseudomorphs and parent silica; effect of autoclaving time and pH adjustment. (For sample identification, see Table 1.)

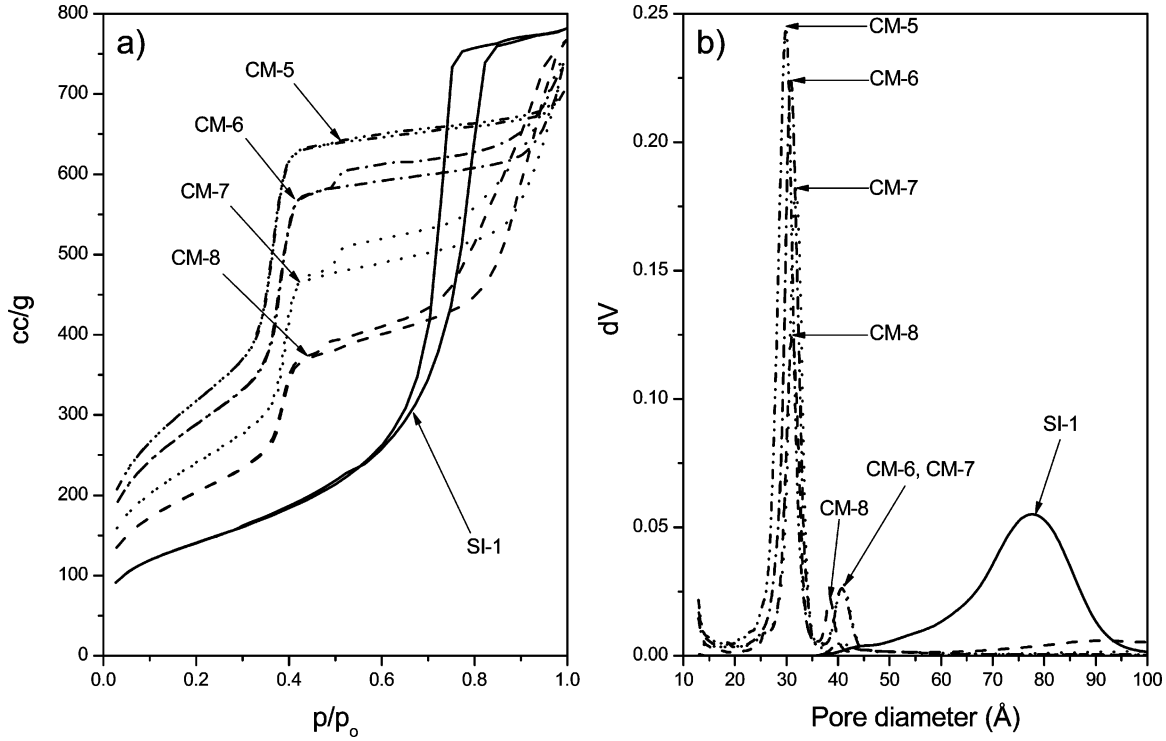

Figure 5. Nitrogen physisorption results of parent silica and Co−MCM-41 pseudomorphs; effect of autoclaving time and pH adjustment. (For sample identification, see Table 1.)

morphic Co−MCM-41 for the same purpose as powder Co−MCM-41, but may allow it to be used in a fluidized-bed reactor.

To investigate the Co species in Co−MCM-41 pseudomorphs and the reduction stability of these samples, hydrogen TPR was carried out on the 4 day autoclaved samples synthesized under different initial pH, and the results are depicted in Figure 7. The initial pH of the synthesis solution significantly affects the reduction stability of Co−MCM-41, and the explanation is tentatively attributed to different locations of Co ions in the MCM-41 framework.[10] That is, increasing initial pH of Co−MCM-41 improves the reduction stability of Co ions because more Co ions could be incorporated in the silica framework of MCM-41 under higher pH. The same reduction stability pattern with the initial pH is noted in Co−MCM-41 pseudomorphs as shown in Figure 7. The reduction peak around 500 °C, reduction of Co^{3+} that is the oxidized form of Co^{2+} in the framework,[11] also increases as the initial pH decreases, which suggests that lowering the initial pH creates more subsurface Co ions

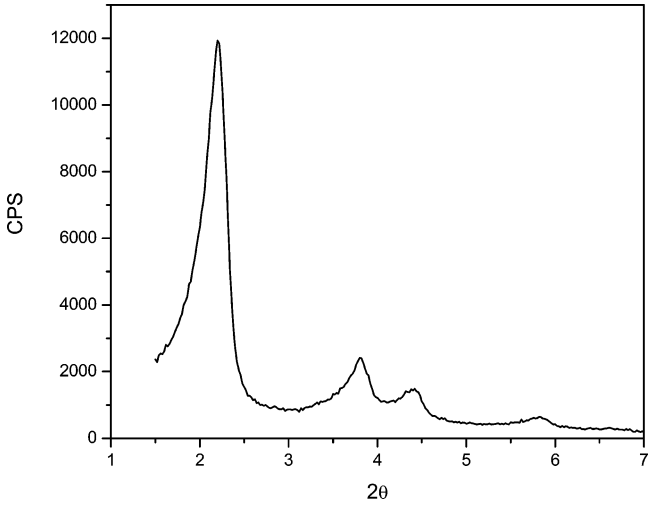

Figure 6. XRD of CM-5 showing the MCM-41 hexagonal pore structure.

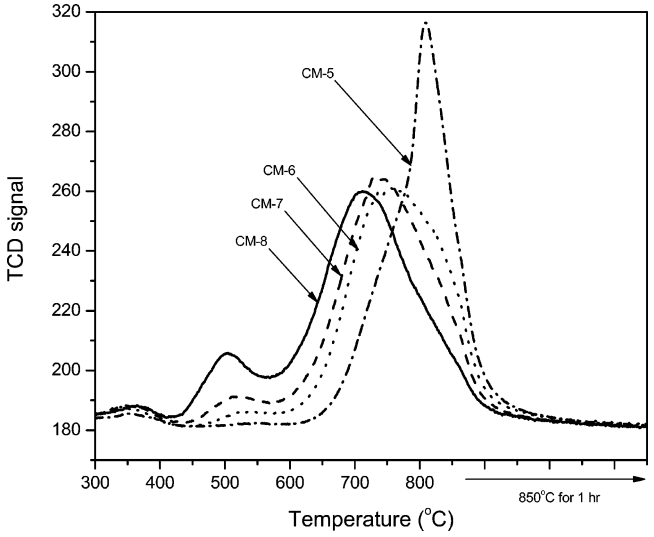

Figure 7. Hydrogen temperature-programmed reduction (TPR) profiles of Co−MCM-41 samples synthesized pseudomorphically; effect of autoclaving time and pH adjustment. (For sample identification, see Table 1.)

Table 2. Bet Surface Area, Pore Volume, and Porosity of the Co−MCM-41 Samples and Parent Silica

		pore volume		
samples	BET area (m^2/g)	mesopore volume (cm^3/g)	total pore volume (cm^3/g)	mesoporosity (%)
SI-1	513	1.24	1.29	96
SI-2	550	0.83	0.87	95
CM-1	361	0.39	0.55	71
CM-2	403	0.37	0.97	38
CM-3	1057	1.00	1.36	74
CM-4	1051	0.98	1.24	79
CM-5	**1159**	**1.11**	**1.18**	**94**
CM-6	**1050**	**1.02**	**1.21**	**84**
CM-7	**872**	**0.87**	**1.21**	**72**
CM-8	**742**	**0.73**	**1.23**	**59**

in the framework, resulting in a greater fraction being oxidized during sample calcination. The sample synthesized at the optimum condition, CM-5, shows the highest reduction stability with narrowest temperature distribution, showing the maximum reduction rate at 800 °C, which corresponds to a shoulder on the high-temperature side of CM-6, without Co^{3+} on the surface, indicating most Co^{2+} ions are distributed in the core of the silica wall.

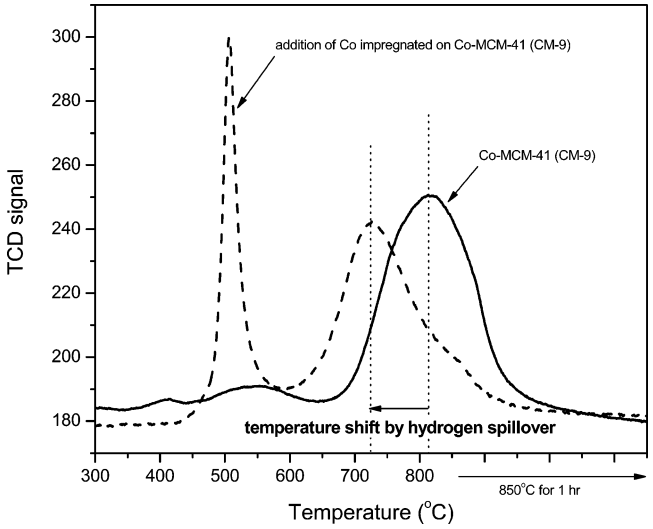

Figure 8. Hydrogen temperature-programmed reduction (TPR) profiles of Co−MCM-41 samples for the explanation of hydrogen spillover effect. (For sample identification, see Table 1.)

A shift of the maximum reduction rate to lower temperature with increased surface compound amount can be noted in Figure 7. The reduction stability was explained earlier,[10] by a different location of Co ions in the framework; however, the relationship between surface compounds and reduction stability cannot be overlooked. The possibility of hydrogen spillover[14] can be hypothesized to explain this relationship. Surface compounds can be reduced at much lower temperature than Co ions of the framework. The low-temperature reduced metallic Co dissociates hydrogen molecules before framework Co ions start to be reduced. The dissociated hydrogen migrates on and into the surface participating in the reduction process of Co ions, resulting in accelerating the reduction rate of Co ions. To obtain evidence for this hypothesis, 0.05 wt % Co (corresponding to 5% of 1 wt % Co in MCM-41) was impregnated on CM-9 using cobalt sulfate ($CoSO_4 \cdot 7H_2O$), and hydrogen TPR was performed with this sample without calcination to avoid cobalt silicate formation on the surface. The reduction patterns before and after addition of Co impregnation are compared in Figure 8. A significant amount of hydrogen consumption around 500 °C is monitored, which might be from reduction of Co sulfate on the surface. This additional surface Co compound shifted the maximum reduction rate of Co ions in the silica matrix about 100 °C lower than that of CM-9. This indicates that there is a hydrogen spillover effect when reducible surface Co compounds coexist with Co ions in the silica matrix.

Conclusion

Pseudomorphic synthesis of Co−MCM-41 using 15 and 40 μm spherical silica particles was successfully performed. Autoclaving time and the initial pH of the synthesis solution were crucial factors for obtaining nonruptured morphology and complete transformation of parent silica large particles to the MCM-41 structure. These factors also affected the distribution of Co ions in the MCM-41 structure, which is the key to some catalytic applications. The optimum auto-

(14) Vannice, M. A.; Neikam, W. C. *J. Catal.* **1971**, *20*, 260.

claving time and the initial pH were 4 days and 12, respectively. The initial pH adjustment of Co−MCM-41 synthesis solution affected the reduction stability by controlling Co ion location in the framework as well as hydrogen spillover on the surface. Finally, the successful application of these large catalytic particles in a fluidized-bed synthesis of SWNT is a realistic prospect utilizing materials synthesized by the process described herein.

Acknowledgment. We are grateful to the DoE, Office of Basic Energy Sciences, Grant No. DE-FG02-01.ER15183, for the financial support of this project. We also thank Dr. Zhenting Jiang, Department of Geology, Yale University, for arranging and helping perform SEM experiments. Partial support by DARPA (Hexcel Corp. subcontract) is also acknowledged.

CM061342S